

ECG strain pattern in hypertension is associated with myocardial cellular expansion and diffuse interstitial fibrosis: a multi-parametric cardiac magnetic resonance study

Jonathan C.L. Rodrigues^{1,2}, Antonio Matteo Amadu^{1,3}, Amardeep Ghosh Dastidar^{1,4}, Bethannie McIntyre⁵, Gergley V. Szantho^{1,6}, Stephen Lyen^{1,7}, Cattleya Godsava⁸, Laura E.K. Ratcliffe⁹, Amy E. Burchell⁹, Emma C. Hart^{2,9}, Mark C.K. Hamilton^{1,7}, Angus K. Nightingale^{1,4,9}, Julian F.R. Paton^{2,9}, Nathan E. Manghat^{1,7*}, and Chiara Bucciarelli-Ducci^{1,4,10*}

¹NIHR Bristol Cardiovascular Biomedical Research Unit, Bristol Heart Institute, University Hospitals Bristol NHS Foundation Trust, Upper Maudlin Street, Bristol BS2 8HW, UK; ²School of Physiology, Pharmacology and Neuroscience, Faculty of Biomedical Sciences, University of Bristol, Bristol, UK; ³Department of Surgical, Microsurgical and Medical Sciences, Institute of Radiology, University of Sassari, Sassari, Italy; ⁴Department of Cardiology, Bristol Heart Institute, University Hospitals Bristol NHS Foundation Trust, Bristol, UK; ⁵Severn Postgraduate Medical Education Foundation School, NHS Health Education South West, Bristol, UK; ⁶Department of Cardiology, University Hospital of Wales, Cardiff, UK; ⁷Department of Radiology, Bristol Royal Infirmary, University Hospitals Bristol NHS Foundation Trust, Bristol, UK; ⁸Department of General Medicine, Bristol Royal Infirmary, University Hospitals Bristol NHS Foundation Trust, Bristol, UK; ⁹CardioNomics Research Group, Clinical Research and Imaging Centre (CRIC) Bristol, Bristol Heart Institute, University Hospitals Bristol NHS Foundation Trust, Upper Maudlin Street, Bristol BS2 8HW; and ¹⁰School of Clinical Sciences, Faculty of Health Sciences, University of Bristol, Bristol, UK

Received 2 March 2016; accepted after revision 8 May 2016; online publish-ahead-of-print 22 June 2016

Aims

In hypertension, the presence of left ventricular (LV) strain pattern on 12-lead electrocardiogram (ECG) carries adverse cardiovascular prognosis. The underlying mechanisms are poorly understood. We investigated whether hypertensive ECG strain is associated with myocardial interstitial fibrosis and impaired myocardial strain, assessed by multi-parametric cardiac magnetic resonance (CMR).

Methods and results

A total of 100 hypertensive patients [50 ± 14 years, male: 58%, office systolic blood pressure (SBP): 170 ± 30 mmHg, office diastolic blood pressure (DBP): 97 ± 14 mmHg] underwent ECG and 1.5T CMR and were compared with 25 normotensive controls (46 ± 14 years, 60% male, SBP: 124 ± 8 mmHg, DBP: 76 ± 7 mmHg). Native T1 and extracellular volume fraction (ECV) were calculated with the modified look-locker inversion-recovery sequence. Myocardial strain values were estimated with voxel-tracking software. ECG strain ($n = 20$) was associated with significantly higher indexed LV mass (LVM) (119 ± 32 vs. 80 ± 17 g/m², $P < 0.05$) and ECV (30 ± 4 vs. 27 ± 3%, $P < 0.05$) compared with hypertensive subjects without ECG strain ($n = 80$). ECG strain subjects had significantly impaired circumferential strain compared with hypertensive subjects without ECG strain and controls (−15.2 ± 4.7 vs. −17.0 ± 3.3 vs. −17.3 ± 2.4%, $P < 0.05$, respectively). In subgroup analysis, comparing ECG strain subjects to hypertensive subjects with elevated LVM but no ECG strain, a significantly higher ECV (30 ± 4 vs. 28 ± 3%, $P < 0.05$) was still observed. Indexed LVM was the only variable independently associated with ECG strain in multivariate logistic regression analysis [odds ratio (95th confidence interval): 1.07 (1.02–1.12), $P < 0.05$].

Conclusion

In hypertension, ECG strain is a marker of advanced LVH associated with increased interstitial fibrosis and associated with significant myocardial circumferential strain impairment.

Keywords

fibrosis • hypertension • hypertrophy • remodelling • myocardial strain • ECG

* Corresponding author. Tel: +44 1173425885; Fax: +44 1173425526. E-mail: c.bucciarelli-ducci@bristol.ac.uk (C.B.-D.); nathan.manghat@uhbristol.nhs.uk (N.E.M.)

© The Author 2016. Published by Oxford University Press on behalf of the European Society of Cardiology.

This is an Open Access article distributed under the terms of the Creative Commons Attribution Non-Commercial License (<http://creativecommons.org/licenses/by-nc/4.0/>), which permits non-commercial re-use, distribution, and reproduction in any medium, provided the original work is properly cited. For commercial re-use, please contact journals.permissions@oup.com

Introduction

The American Joint National Committee on Prevention, Detection, Evaluation, and Treatment of High Blood Pressure¹ and the 2013 joint European Society of Hypertension/European Society of Cardiology² advise that a 12-lead electrocardiogram (ECG) be routinely performed in all patients with arterial hypertension. In hypertension, left ventricular (LV) ECG strain is a powerful predictor of myocardial infarction (MI) and cardiovascular death.³ It is also a significant independent predictor for the development of, and death from, congestive cardiac failure.⁴ Furthermore, the development of ECG strain in the context of anti-hypertensive therapy is independently associated with cardiovascular death, MI, stroke, sudden cardiac death, and all-cause mortality.⁵ However, the mechanisms of the characteristic ST-segment and T-wave changes in hypertensive ECG strain are unknown.

Interstitial myocardial fibrosis has been documented histologically in hypertensive subjects at post-mortem⁶ and at biopsy.⁷ Native T1 mapping is a non-contrast, non-invasive cardiac magnetic resonance (CMR) technique that can determine whether myocardial structural changes exist at the intracellular and/or extracellular level.^{8,9} Using both native and post-contrast T1 mapping, such myocardial changes can be localized to the myocardial interstitium by calculating the myocardial extracellular volume fraction (ECV). CMR T1 mapping sequences have been histologically validated in *ex vivo* human hearts following cardiac transplantation,¹⁰ and the techniques can reliably detect and quantify myocardial interstitial fibrosis.

The pathophysiological association between myocardial interstitial fibrosis, as assessed with CMR T1 mapping, LV mechanics and ECG strain in hypertensive patients, remains poorly understood and was investigated in the present study. We hypothesized that ECG strain would be associated with diffuse myocardial interstitial fibrosis and with myocardial systolic dysfunction.

Methods

Study subjects

Patients with hypertension were prospectively recruited from the Bristol Heart Institute tertiary hypertension clinic between February 2012 and January 2016. The local research ethics committee confirmed that the study conformed to the governance arrangements for research ethics committees. Written consent was provided. Demographic and clinical characteristics were documented. Exclusion criteria consisted of evidence of any concurrent myocardial pathology (e.g. moderate–severe valvular heart disease and inherited/acquired cardiomyopathies) and severely decreased estimated glomerular filtration rate (eGFR) <30 mL/min/1.73 m², precluding the use of gadolinium-chelate contrast agent. Normotensive healthy volunteers acted as a control group.

Average office systolic (SBP) and diastolic blood pressures (DBP) were obtained with an appropriately sized brachial cuff in all subjects after seated rest from both arms, assessed using standard automated sphygmomanometry.¹¹

Electrocardiographic analysis

A 12-lead ECG (scale: 10 mm = 1 mV, speed: 25 mm/s) was acquired supine during gentle respiration in all hypertensive subjects. ECG strain was defined as ≥ 1 mm concave down-sloping ST-segment depression

and asymmetrical T-wave inversion in the lateral leads, as previously described.¹² Complete bundle branch block or digoxin confounded analysis, necessitating exclusion. ECG interpretation was performed by an experienced clinician, blinded to both other clinical and CMR data.

CMR cine protocol and analysis

CMR was performed at 1.5T (Avanto, Siemens, Erlangen, Germany). Steady-state free precession (SSFP) short-axis cines for the LV (slice thickness: 8 mm, no inter-slice gap, temporal resolution: 38.1 ms, echo time: 1.07 ms, in-plane pixel size: 1.5 × 0.8 mm) were used to calculate LV mass (LVM) and volumes, which were subsequently indexed to body surface area as previously described.¹³ As per the Society for CMR guidelines,¹⁴ a validated¹⁵ threshold-detection software (CMR42, Circle Cardiovascular Imaging Inc., Calgary, Canada) was used, enabling papillary muscles and LV trabeculae to be included in the estimation of LVM. Left ventricular hypertrophy (LVH) was defined as indexed LVM >95th percentile of widely used CMR normal ranges (men: 89–93 g/m² and women: 77–78 g/m² depending on age).¹³ The CMR-derived mass-to-volume ratio (M/V), akin to the echocardiographic measure of relative wall thickness,¹⁶ was documented. Patterns of LVH were defined as concentric LVH where there was elevated indexed LVM but normal indexed EDV and eccentric LVH where there was an elevated indexed LVM and concomitant elevated indexed EDV relative to normal reference ranges,¹³ in a manner similar to previously described echocardiographic¹⁷ and CMR¹⁶ studies of LV phenotypes. The CMR volumetrics were performed by an experienced CMR reader, who was blinded to all other data.

CMR late gadolinium protocol and analysis

Replacement myocardial fibrosis was assessed by late gadolinium enhancement (LGE).¹⁸ An inversion-recovery fast gradient recall echo sequence performed, in two phase-encoding directions where necessary, was used 10–15 min after the administration of 0.1 mmol/kg gadobutrol (Gadovist, Bayer Pharma AG, Germany) intravenously. The inversion time was optimized to achieve nulling of normal myocardium. LGE assessment was visual consensus between two expert CMR readers, blinded to clinical and ECG data. Any patients exhibiting any type of LGE were excluded to avoid confounding effects of replacement fibrosis. Normotensive control subjects did not receive intravenous gadolinium-chelate.

CMR T1 mapping protocol and analysis

Myocardial T1 mapping was performed using the modified look-locker inversion-recovery (MOLLI) sequence [flip angle: 35°, minimum time to inversion (TI): 100 ms, T1 increment: 80 ms, time delay: 150 ms, heart beat acquisition scheme: 5-(3)-3].¹⁹ Regions of interest (ROI) were drawn within the mid-septum on short-axis, motion-corrected native T1 maps and copied onto corresponding 15-min post-contrast maps, with minor adjustments to minimize partial volume artefact, as previously described.²⁰ T1 analysis was performed with Argus software (Siemens, Erlangen, Germany), as previously described.²¹ The T1 values were the mean of all pixels within the ROI. Analysis was performed by an experienced CMR reader, blinded to all other data. The ECV was calculated as²⁰: $ECV = (\Delta R1_{\text{myocardium}} / \Delta R1_{\text{blood-pool}}) \times (1 - \text{haematocrit})$, where $\Delta R1 = (1/\text{post-contrast T1} - 1/\text{native T1})$. Myocardial cell volume fraction was defined, as previously,²² as $1 - ECV$ and multiplied by indexed myocardial volume (indexed LVM divided by 1.05 g/mL, the myocardial specific gravity). Indexed interstitial volume was defined as $ECV \times \text{indexed myocardial volume}$. This T1 technique analysis has previously been demonstrated to yield high reproducibility.^{21,23}

CMR strain imaging

Strain imaging was performed with voxel-tracking post-processing software (Tissue Tracking, CMR42, Circle Cardiovascular Imaging Inc., Calgary, Canada) on two-chamber, four-chamber, and short-axis stack SSFP cine images by defining endocardial and epicardial borders (excluding papillary muscles and trabeculae) and the mitral valve annular plane at end-diastole. Global longitudinal strain was the averaged strain from four-chamber and two-chamber analysis. Circumferential and radial strain were calculated as mean values of mid-myocardial segments from the short-axis cine two-dimensional (2D) strain model, in order to minimize partial voluming and through-plane motion at the base and apex. The software tracks every myocardial voxel through the cardiac cycle in 2D. It is based on a previously described algorithm.^{24,25} Strain data from hypertensive subjects were compared with data from normotensive controls. All strain analysis was performed by an experienced CMR reader blinded to all other data.

Statistical analysis

Statistical analysis was performed using SPSS v.21 (IBM Corp., Armonk, NY, USA). Categorical variables were analysed using the Fisher's exact test. Continuous variables were expressed as mean \pm standard deviation, and normally distributed variables were compared using one-way analysis of variance with least significant difference *post hoc* correction for multiple testing. Determinates of ECG strain were assessed by univariate and multivariate logistic regression models. Significance was defined as two-tailed $P < 0.05$.

Results

Demographics

Of the 130 eligible hypertensive subjects, 30 were excluded (Figure 1) resulting in a final hypertensive sample size of 100 (age: 50 ± 14 years, male: 58%, office SBP: 170 ± 30 mmHg, office DBP: 97 ± 14 mmHg).

Twenty-five healthy control subjects were recruited (age: 46 ± 14 years, male: 60%, office SBP: 124 ± 8 mmHg, office DBP: 76 ± 7 mmHg). There were no significant racial differences between the study subgroups. On the basis of LGE, six hypertensive subjects were excluded: one had subepicardial non-*ischaemic* LGE suggesting previous myocarditis, two had subendocardial *ischaemic* LGE, and three had mid-wall fibrosis and ancillary clinical/CMR findings suggestive of concomitant hypertrophic cardiomyopathy.

Prevalence of ECG strain

ECG strain was present in 20% ($n = 20$) of hypertensive subjects (Table 1). The prevalence of diabetes was higher in hypertensive subjects with ECG strain compared with those without ECG strain (25 vs. 9%, $P < 0.05$). Subjects with ECG strain were prescribed significantly more anti-hypertensive agents (4 ± 3 vs. 2 ± 2 , $P < 0.05$). There were no other significant demographic differences between the subgroups.

Myocardial structural changes in ECG strain

Those subjects with ECG strain had significantly higher indexed LVM compared with those without ECG strain (119 ± 32 vs. 80 ± 17 g/m², $P < 0.05$), which was a result of significant increases in both indexed myocardial volume (82 ± 21 vs. 56 ± 12 mL/m², $P < 0.05$) and indexed interstitial volume (36 ± 13 vs. 21 ± 5 mL/m², $P < 0.05$) (Table 2, Figures 2 and 3).

Myocardial functional changes in ECG strain

Despite no significant differences in left ventricular ejection fraction (LVEF), subjects with ECG strain had significantly reduced

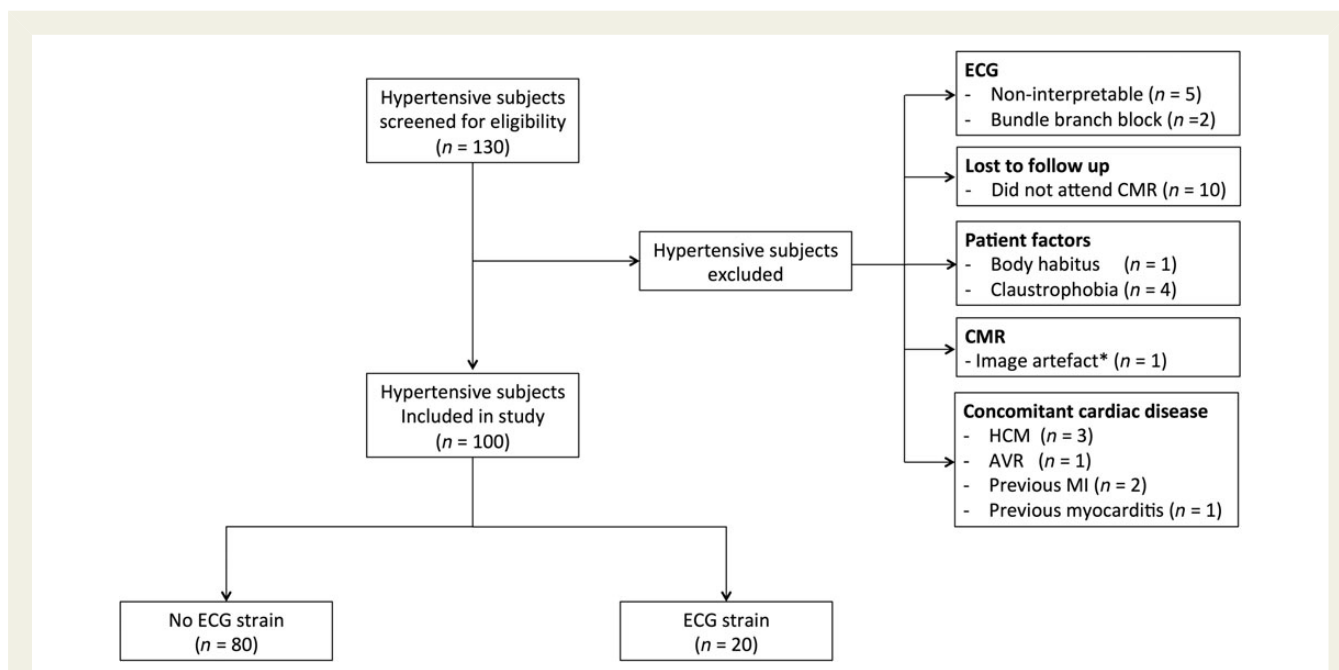


Figure 1 A flow chart describing the reasons for exclusion and final hypertensive sample size ($n = 100$). * Images degraded by implantable loop recorder.

Table 1 Demographic data for hypertensive subjects and normotensive controls

	Controls (n = 25)	Hypertensive subjects (n = 100)	
		No ECG strain (n = 80)	ECG strain (n = 20)
Age (years)	46 ± 14 ^a	49 ± 14	55 ± 13
Gender (% male)	60	55	70
Ethnicity (% Caucasian)	93	81	85
BMI (kg/m ²)	26 ± 5 ^b	30 ± 6	31 ± 4
Diabetes (%)	0	9	25 ^c
Heart rate (bpm)	66 ± 12	72 ± 12	66 ± 11
Office SBP (mmHg)	124 ± 8 ^b	166 ± 30	186 ± 27 ^c
Office DBP (mmHg)	76 ± 7 ^b	97 ± 14	97 ± 12
ESH/ESC office BP grade ^e			
Controlled (%)		9	0
High normal (%)		5	0
Grade 1 (%)		27	25
Grade 2 (%)		25	20
Grade 3 (%)		31	50
Isolated systolic HTN (%)		3	5
No. of anti-hypertensive medications	0	2 ± 2	4 ± 3 ^d
ACEi/ARB (%)	0	75	85

^aControls vs. ECG strain, $P < 0.05$.

^bControls vs. all other subgroups, $P < 0.05$.

^cECG strain vs. all other subgroups, $P < 0.05$.

^dECG strain vs. no ECG strain, $P < 0.05$.

^eEuropean Society of Hypertension/European Society of Cardiology (ESH/ESC) Office BP grade: controlled SBP: 120–129 and/or DBP: 80–84; high normal SBP: 130–139 and/or DBP: 85–89; Grade 1 SBP: 140–159 and/or DBP: 90–99; Grade 2 SBP: 160–179 and/or DBP: 100–109; Grade 3 SBP: ≥180 and/or DBP: ≥110; isolated systolic hypertension SBP: ≥140 and DBP: <90.

Table 2 CMR volumetric, T1 mapping, and myocardial strain data for hypertensive subjects and normotensive controls

	Controls (n = 25)	Hypertensive subjects (n = 100)	
		No ECG strain (n = 80)	ECG strain (n = 20)
LV volumetrics			
Ejection fraction (%)	64 ± 5	67 ± 8	66 ± 13
Indexed EDV (mL/m ²)	79 ± 18	75 ± 17	84 ± 18
Indexed ESV (mL/m ²)	29 ± 8	26 ± 12	30 ± 16
Indexed SV (mL/m ²)	50 ± 11	50 ± 11	58 ± 10 ^a
Indexed LVM (g/m ²)	61 ± 11 ^b	80 ± 17	119 ± 32 ^c
Mass-to-volume ratio (g/mL)	0.80 ± 0.12 ^b	1.11 ± 0.30 ^b	1.44 ± 0.35 ^c
T1 mapping			
Native T1 (ms)	1026 ± 41	1035 ± 37	1070 ± 46 ^c
Extracellular volume fraction (%)	–	27 ± 3	30 ± 4 ^a
Myocardial cell volume fraction (%)	–	73 ± 3	70 ± 4 ^a
Indexed interstitial volume (mL/m ²)	–	21 ± 5	36 ± 13 ^a
Indexed myocardial cell volume (mL/m ²)	–	56 ± 12	82 ± 21 ^a
Myocardial strain function			
Peak circumferential strain (%)	–17.3 ± 2.4	–17.0 ± 3.3	–15.2 ± 4.7 ^c
Peak longitudinal strain (%)	–17.8 ± 2.6	–16.8 ± 2.8	–15.9 ± 4.5 ^d
Peak radial strain (%)	28.6 ± 5.7	29.0 ± 8.6	25.6 ± 11.1

^aECG strain vs. no ECG strain, $P < 0.05$.

^bControls vs. all subgroups, $P < 0.05$.

^cECG strain vs. all subgroups, $P < 0.05$.

^dECG strain vs. controls, $P < 0.05$.

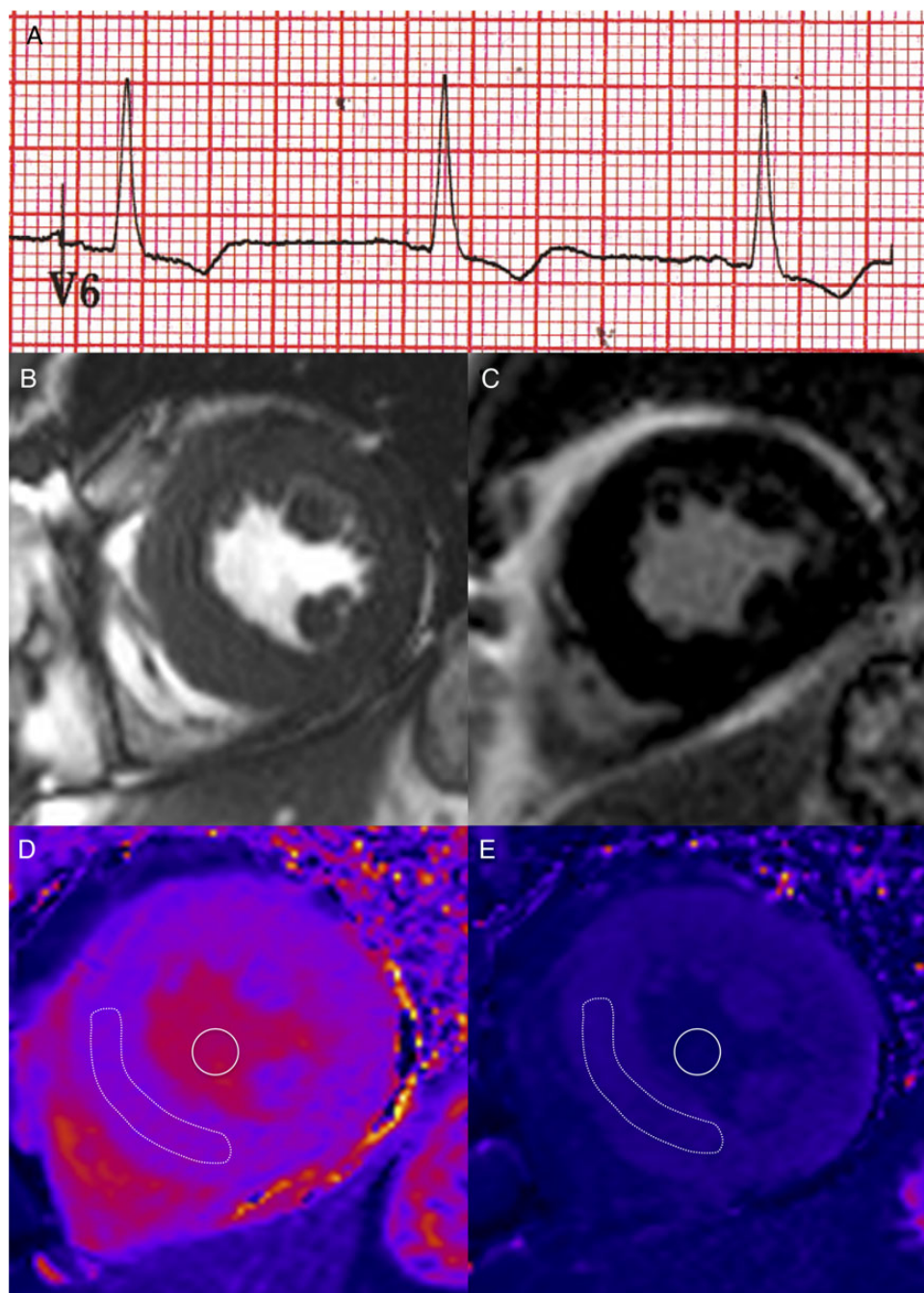


Figure 2 Representative example of a hypertensive subject with ECG strain. (A) Evidence of ECG strain. (B) SSFP short-axis cine image at end-diastole. Indexed LVM = 153 g/m^2 . (C) LGE image showing no replacement fibrosis. (D) Native T1 map. Mean T1 relaxation time of myocardium = 1081 ms and of blood pool = 1595 ms. (E) Post-contrast T1 map. Mean T1 relaxation time of myocardium = 433 ms and of blood pool = 319 ms. ECV = 32%.

circumferential strain (-15.2 ± 4.7 vs. -17.0 ± 3.3 vs. $-17.3 \pm 2.4\%$, $P < 0.05$, respectively) compared with both hypertensive subjects without ECG strain and normotensive subjects. Similar nonsignificant trends were demonstrated for longitudinal and radial strain between the cohorts (Figure 4).

Hypertensive ECG strain subjects vs. hypertensive subjects without ECG strain but with elevated indexed LVM

In this hypertensive subgroup analysis, subjects with ECG strain had significantly higher indexed LVM (119 ± 32 vs. $100 \pm 14 \text{ g/m}^2$,

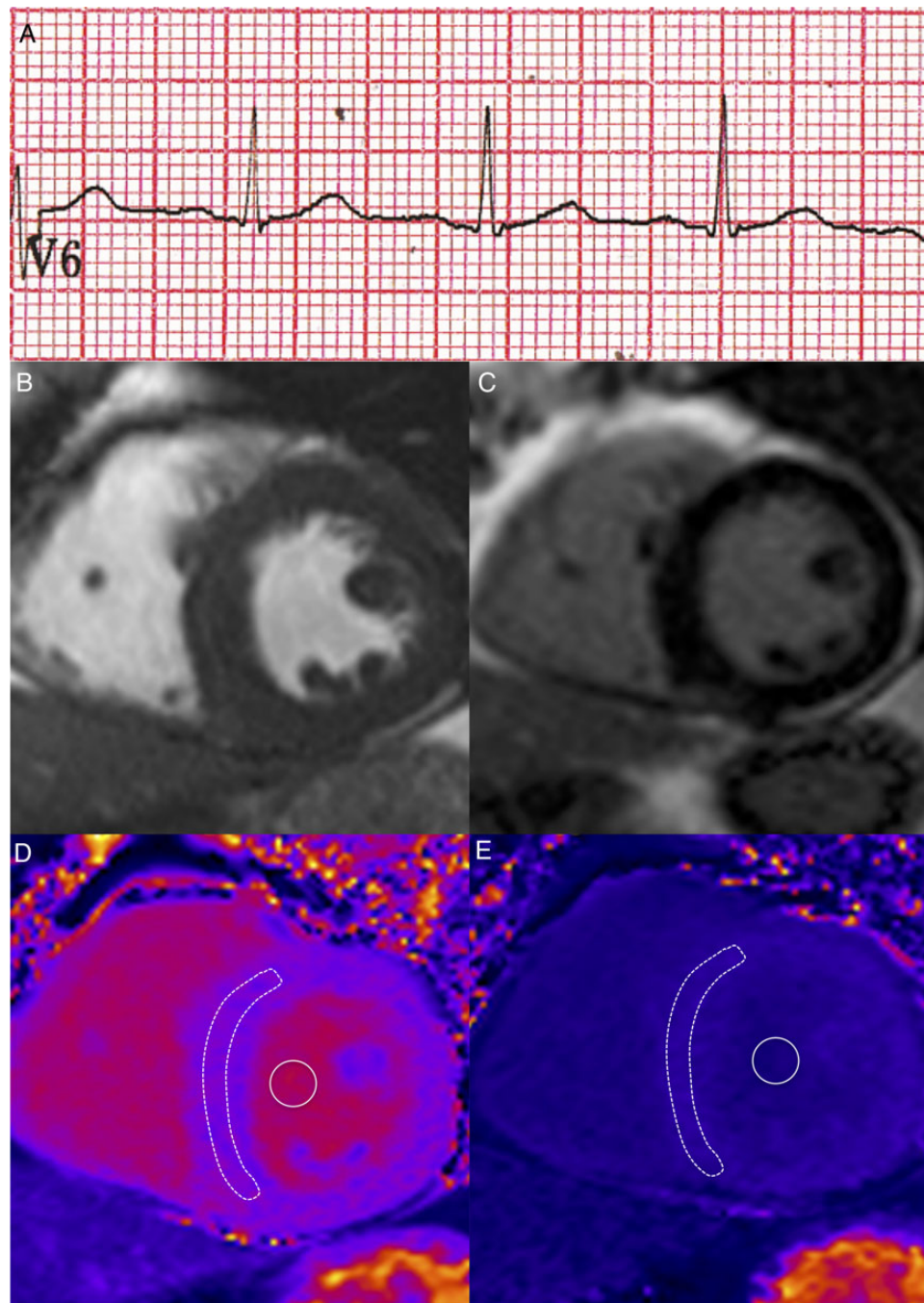


Figure 3 Representative example of a hypertensive subject with LVH but no ECG strain. (A) No evidence of ECG strain. (B) SSFP short-axis cine image at end-diastole. Indexed LVM = 92 g/m^2 . (C) LGE image showing no replacement fibrosis. (D) Native T1 map. Mean T1 relaxation time of myocardium = 1033 ms and of blood pool = 1653 ms. (E) Post-contrast T1 map. Mean T1 relaxation time of myocardium = 520 ms and of blood pool = 368 ms. ECV = 27%.

$P < 0.05$), ECV (30 ± 4 vs. $28 \pm 3\%$, $P < 0.05$), indexed myocardial cell volume (82 ± 21 vs. $68 \pm 11 \text{ mL/m}^2$, $P < 0.05$), and indexed interstitial volume (36 ± 13 vs. $27 \pm 5 \text{ mL/m}^2$, $P < 0.05$) compared with hypertensive subjects with LVH but without ECG strain (Table 3).

In terms of LV geometry, subjects with ECG strain had significantly higher M/V compared with those with LVH but no ECG strain

(1.44 ± 0.35 vs. $1.11 \pm 0.30 \text{ g/mL}$, $P < 0.05$). However, there was no significant difference in the prevalence of pattern of LVH (concentric LVH: 55 vs. 70%, $P = 0.24$ and eccentric LVH: 20 vs. 30%, $P = 0.30$) geometry between subjects with ECG strain and those with LVH but no ECG strain.

Functionally, those with ECG strain demonstrated trends towards more severe myocardial strain impairment in circumferential

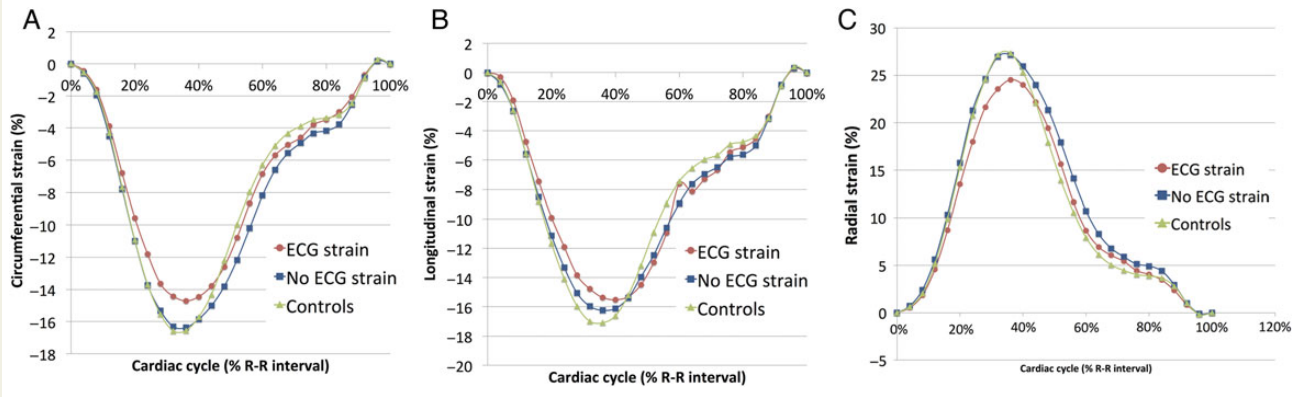


Figure 4 Graphs of (A) mean circumferential strain of the mid-myocardium, (B) mean global longitudinal strain, and (C) mean radial strain of the mid-myocardium over the cardiac cycle for normotensive control and hypertensive (ECG strain and no ECG strain) cohorts.

Table 3 CMR volumetric, T1 mapping, and myocardial strain data for hypertensive subgroup analysis

	No ECG strain (n = 80)		ECG strain (n = 20)
	No LVH (n = 56)	LVH (n = 24)	
Demographics			
Age (years)	47 ± 15	51 ± 13	55 ± 13 ^a
Gender (% male)	48	71	70
BMI (kg/m ²)	30 ± 6	31 ± 6	31 ± 4
Diabetes (%)	7	13	25 ^a
Office SBP (mmHg)	164 ± 28	170 ± 34	186 ± 27 ^a
Office DBP (mmHg)	94 ± 12	103 ± 15 ^b	97 ± 12
LV volumetrics			
Ejection fraction (%)	69 ± 7	64 ± 10 ^b	66 ± 13
Indexed EDV (mL/m ²)	71 ± 15 ^c	86 ± 17	84 ± 18
Indexed ESV (mL/m ²)	22 ± 8 ^c	33 ± 15	30 ± 16
Indexed SV (mL/m ²)	48 ± 10 ^c	54 ± 11	56 ± 15
Indexed LVM (g/m ²)	72 ± 10 ^c	100 ± 14	119 ± 32 ^d
Mass-to-volume ratio (g/mL)	1.05 ± 0.27 ^c	1.24 ± 0.35	1.44 ± 0.36 ^d
T1 mapping			
Native T1 (ms)	1030 ± 38	1047 ± 35	1070 ± 46 ^a
Post-contrast T1 (ms)	543 ± 49	551 ± 36	511 ± 70 ^d
Extracellular volume fraction (%)	27 ± 3	28 ± 3	30 ± 4 ^a
Myocardial cell volume fraction (%)	73 ± 3	72 ± 4	70 ± 4 ^a
Indexed interstitial volume (mL/m ²)	18 ± 3 ^c	27 ± 5	36 ± 13 ^d
Indexed myocardial cell volume (mL/m ²)	50 ± 8 ^c	68 ± 11	82 ± 21 ^d
Myocardial strain function			
Peak circumferential strain (%)	-17.5 ± 2.9 ^c	-15.7 ± 3.7	-15.2 ± 4.8
Peak longitudinal strain (%)	-17.2 ± 2.2 ^c	-15.7 ± 3.7	-15.9 ± 3.7
Peak radial strain (%)	30.1 ± 8.2	26.3 ± 9.2	25.6 ± 11.1

^aECG strain vs. no ECG strain and no LVH, $P < 0.05$.

^bNo ECG strain and LVH vs. no ECG strain and no LVH, $P < 0.05$.

^cNo ECG strain and no LVH vs. all subgroups, $P < 0.05$.

^dECG strain vs. all subgroups, $P < 0.05$.

Table 4 Univariate and multivariate logistic regression analyses to assess determinants of ECG strain

	Univariate analysis		Multivariate analysis	
	OR (95% CI)	P-value	OR (95% CI)	P-value
Age (years)	1.03 (0.99–1.07)	0.08	0.96 (0.94–1.08)	0.99
Male gender	1.91 (0.67–5.47)	0.23	–	–
Presence of diabetes	3.48 (0.97–12.44)	0.06	1.18 (0.15–9.52)	0.87
Office SBP (mmHg)	1.02 (1.01–1.04)	<0.05	1.02 (0.99–1.06)	0.15
Indexed LVM (g/m ²)	1.08 (1.04–1.10)	<0.0001	1.07 (1.03–1.11)	<0.005
Indexed EDV (mL/m ²)	1.03 (0.99–1.06)	0.06	1.00 (0.94–1.05)	0.87
Native T1 (ms)	1.02 (1.01–1.04)	<0.01	1.00 (0.97–1.02)	0.82
ECV (%)	1.24 (1.05–1.46)	<0.05	1.06 (0.82–1.38)	0.64

OR, odds ratio; CI, confidence interval; LVM, Left ventricular mass; EDV, end-diastolic volume; ECV, extracellular volume.

and radial deformation directions compared with subjects with LVH but no ECG strain.

Predictors of ECG strain

On univariate logistic regression analysis, indexed LVM, office SBP, native T1, and ECV demonstrated significant association with ECG strain (Table 4). Both indexed myocardial cell volume [odds ratio (95% confidence interval): 1.10 (1.05–1.15), $P < 0.0001$] and indexed interstitial volume [1.21 (1.11–1.33), $P < 0.0001$] were univariate predictors of ECG strain. However, only indexed LVM remained a significant independent determinant in the multivariate logistic regression statistical model, which accounted for age, gender, office SBP, and presence of diabetes.

Discussion

To our knowledge, this is the first study to investigate the pathophysiology of ECG strain in hypertension with advanced CMR multiparametric T1 mapping and voxel-tracking techniques. Our novel findings are that ECG strain pattern in hypertensive subjects is associated with significant increased LVM that is not simply a result of myocardial cellular expansion but due to significantly increased interstitial fibrosis. Subjects with ECG strain have significantly more interstitial fibrosis compared with all subjects without ECG strain and compared with the subgroup of hypertensive patients with LVH but without ECG strain. ECG strain is associated with significantly impaired circumferential strain, despite normal LVEF, compared with those without ECG strain and normotensive controls.

ECG strain and myocardial structure

Indexed LVM was a significant independent predictor of ECG strain in multivariate logistic regression analysis. It is interesting to contrast our findings from a purely hypertensive cohort with patients with aortic stenosis.²⁰ Shah et al. demonstrated similar findings in terms of elevated LVM and ECV in an aortic stenosis subgroup with ECG strain.²⁰ However, in aortic stenosis, increased myocardial fibrosis (either replacement or interstitial), but not increased indexed LVM, maintained an independent association with ECG strain in multivariate analysis. There was also a high prevalence of mid-wall

replacement fibrosis among the aortic stenosis patients. These latter findings contrast with our results and suggest the myocardial response to increased afterload differs in these two disease states, with a predilection for hypertrophy in hypertension and potentially cardiomyopathy in aortic stenosis. However, it is important to realize that hypertension was present in 65% of patients with aortic stenosis and ECG strain in the aforementioned study confounding the comparison.

ECG strain and myocardial function

We also explored the functional implications of identifying ECG strain with CMR myocardial strain analysis. Despite no significant reduction in LVEF, the hypertensive cohort with ECG strain exhibited systolic impairment in all three deformational directions compared with both hypertensive subjects without ECG strain and normotensive controls. Myocardial strain impairment in hypertension has been described in echocardiographic²⁶ and CMR studies.²⁷ It is not possible to determine whether the expansion in myocardial cell volume or the interstitial volume expansion is the predominant factor driving the myocardial impairment in subjects with ECG strain. Both variables are likely to be important. Interstitial fibrosis may result in increased LV stiffness, reduced end-diastolic muscle fibre length, and, therefore, reduced myocardial systolic strain.²⁸ Equally, myocardial cell volume expansion, resulting in increased end-diastolic wall thickness, may mean that less endocardial displacement is required to generate an adequate stroke volume.²⁹ Interestingly, our results suggest that changes in myocardial structure at the intra- and extracellular level appear to predominantly affect the function of the mid-wall circumferential fibres as circumferential strain was the only strain parameter to be significantly impaired in ECG strain subjects compared with all other subgroups.

Left ventricular hypertrophy

Our study also demonstrates that, even in the absence of ECG strain, hypertensive LVH is associated with significantly elevated native T1 compared with normotensive controls. These findings are consistent work by Treibel et al. of 40 hypertensive subjects³⁰ and by Kuruvilla et al. in their study of 43 hypertensive subjects.³¹ We have demonstrated geometrical differences between subjects

with ECG strain and those with LVH but no ECG strain in terms of higher M/V. However, we did not find a significant difference in the prevalence of concentric and eccentric LVH phenotypes.

Limitations

Gadolinium was not administered to the normotensive control group due to lack of ethical approval. As a result, there is no ECV data for the controls in our study. However, the lack of significant difference between native T1 values between controls and hypertensive subjects without LVH suggests that there is a normal ECV in this hypertensive subgroup, which essentially acts as the hypertensive control group.

Despite our study of 100 hypertensive subjects constituting the largest study to date of T1 mapping in hypertension, we did not have sufficient statistical power to determine the impact of hypertension duration on the variables investigated. Diabetes was more common in subjects with ECG strain and can affect cardiac structure and may be a confounding factor.³² However, the presence of diabetes was not a significant predictor of ECG strain in either univariate or multivariate logistic regression analysis.

Conclusion

The most widely applicable finding from our study is that the ECG, a simple, cheap, readily interpretable investigation performed ubiquitously in hypertensive subjects, is a marker of advanced LVH associated with increased interstitial fibrosis and with significant myocardial circumferential strain impairment despite normal LVEF. Further study is now required to determine whether these patients will benefit from aggressive anti-hypertensive, in particular anti-fibrotic, therapies.

Acknowledgements

We thank Mr Christopher Lawton and all the CMR radiographers in the Bristol Heart Institute for their expertise in performing the CMR studies.

Conflict of interest: C.B.-D. is a consultant for Circle Cardiovascular Imaging Inc.

Funding

This work was supported by the Bristol NIHR Cardiovascular Biomedical Research Unit at the Bristol Heart Institute. The views expressed are those of the authors and not necessarily those of the National Health Service, National Institute for Health Research, or Department of Health. J.C.L.R. is funded by the Clinical Society of Bath Postgraduate Research Bursary and Royal College of Radiologists Kodak Research Scholarship. E.C.H. is funded by British Heart Foundation grant IBSRF/FS/11/1/28400. J.F.R.P. is funded by the British Heart Foundation.

References

- Chobanian AV, Bakris GL, Black HR, Cushman WC, Green LA, Izzo JL et al. Seventh report of the Joint National Committee on Prevention, Detection, Evaluation, and Treatment of High Blood Pressure. *Hypertension* 2003;**42**:1206–52.
- Mancia G, Fagard R, Narkiewicz K, Redon J, Zanchetti A, Böhm M et al. 2013 ESH/ESC guidelines for the management of arterial hypertension: the Task Force for the Management of Arterial Hypertension of the European Society of Hypertension (ESH) and of the European Society of Cardiology (ESC). *Eur Heart J* 2013;**34**:2159–219.
- Okin PM, Devereux RB, Nieminen MS, Jern S, Oikarinen L, Viitasalo M et al. Electrocardiographic strain pattern and prediction of cardiovascular morbidity and mortality in hypertensive patients. *Hypertension* 2004;**44**:48–54.
- Okin PM, Devereux RB, Nieminen MS, Jern S, Oikarinen L, Viitasalo M et al. Electrocardiographic strain pattern and prediction of new-onset congestive heart failure in hypertensive patients: the Losartan Intervention for Endpoint Reduction in Hypertension (LIFE) study. *Circulation* 2006;**113**:67–73.
- Okin PM, Oikarinen L, Viitasalo M, Toivonen L, Kjeldsen SE, Nieminen MS et al. Prognostic value of changes in the electrocardiographic strain pattern during anti-hypertensive treatment: the Losartan Intervention for End-Point Reduction in Hypertension Study (LIFE). *Circulation* 2009;**119**:1883–91.
- Rossi MA. Pathologic fibrosis and connective tissue matrix in left ventricular hypertrophy due to chronic arterial hypertension in humans. *J Hypertens* 1998;**16**:1031–41.
- Querejeta R, Varo N, López B, Larman M, Artiñano E, Etayo JC et al. Serum carboxy-terminal propeptide of procollagen type I is a marker of myocardial fibrosis in hypertensive heart disease. *Circulation* 2000;**101**:1729–35.
- Flett AS, Hayward MP, Ashworth MT, Hansen MS, Taylor AM, Elliott PM et al. Equilibrium contrast cardiovascular magnetic resonance for the measurement of diffuse myocardial fibrosis: preliminary validation in humans. *Circulation* 2010;**122**:138–44.
- Bulluck H, Maestrini V, Rosmini S, Abdel-Gadir A, Treibel TA, Castelletti S et al. Myocardial T1 mapping. *Circ J* 2015;**79**:487–94.
- Miller CA, Naish JH, Bishop P, Coutts G, Clark D, Zhao S et al. Comprehensive validation of cardiovascular magnetic resonance techniques for the assessment of myocardial extracellular volume. *Circ Cardiovasc Imaging* 2013;**6**:373–83.
- Beevers G, Lip GY, O'Brien E. ABC of hypertension. Blood pressure measurement. Part 1: sphygmomanometry: factors common to all techniques. *BMJ* 2001;**322**:981–5.
- Hancock EW, Deal BJ, Mirvis DM, Okin P, Kligfield P, Gettes LS et al. AHA/ACC/HRS recommendations for the standardization and interpretation of the electrocardiogram, Part V: electrocardiogram changes associated with cardiac chamber hypertrophy: a scientific statement from the American Heart Association Electrocardiography. *J Am Coll Cardiol* 2009;**53**:992–1002.
- Maceira A, Prasad S, Khan M, Pennell D. Normalized left ventricular systolic and diastolic function by steady state free precession cardiovascular magnetic resonance. *J Cardiovasc Magn Reson* 2006;**8**:417–26.
- Schulz-Menger J, Bluemke DA, Bremerich J, Flamm SD, Fogel MA, Friedrich MG et al. Standardized image interpretation and post processing in cardiovascular magnetic resonance: Society for Cardiovascular Magnetic Resonance (SCMR) Board of Trustees Task Force on Standardized Post Processing. *J Cardiovasc Magn Reson* 2013;**15**:35.
- Childs H, Ma L, Ma M, Clarke J, Cocker M, Green J et al. Comparison of long and short axis quantification of left ventricular volume parameters by cardiovascular magnetic resonance, with ex-vivo validation. *J Cardiovasc Magn Reson* 2011;**13**:40.
- Dweck MR, Joshi S, Murigu T, Gulati A, Alpendurada F, Jabbour A et al. Left ventricular remodeling and hypertrophy in patients with aortic stenosis: insights from cardiovascular magnetic resonance. *J Cardiovasc Magn Reson* 2012;**14**:50.
- Ganau A, Devereux RB, Roman MJ, de Simone G, Pickering TG, Saba PS et al. Patterns of left ventricular hypertrophy and geometric remodeling in essential hypertension. *J Am Coll Cardiol* 1992;**19**:1550–8.
- Mahrholdt H, Wagner A, Judd RM, Sechtum U, Kim RJ. Delayed enhancement cardiovascular magnetic resonance assessment of non-ischaemic cardiomyopathies. *Eur Heart J* 2005;**26**:1461–74.
- Messroghli DR, Greiser A, Fröhlich M, Dietz R, Schulz-Menger J. Optimization and validation of a fully-integrated pulse sequence for modified look-locker inversion-recovery (MOLLI) T1 mapping of the heart. *J Magn Reson Imaging* 2007;**26**:1081–6.
- Shah AS, Chin CWL, Vassiliou V, Cowell SJ, Doris M, Kwok TC et al. Left ventricular hypertrophy with strain and aortic stenosis. *Circulation* 2014;**130**:1607–16.
- Pica S, Sado DM, Maestrini V, Fontana M, White SK, Treibel T et al. Reproducibility of native myocardial T1 mapping in the assessment of Fabry disease and its role in early detection of cardiac involvement by cardiovascular magnetic resonance. *J Cardiovasc Magn Reson* 2014;**16**:99.
- Flett AS, Sado DM, Quarta G, Mirabel M, Pellerin D, Herrey AS et al. Diffuse myocardial fibrosis in severe aortic stenosis: an equilibrium contrast cardiovascular magnetic resonance study. *Eur Heart J Cardiovasc Imaging* 2012;**13**:819–26.
- Roujol S, Weingartner S, Foppa M, Chow K, Kawaji K, Kissinger KV et al. Accuracy and reproducibility of four T1 mapping sequences: a head-to-head comparison of MOLLI, ShMOLLI, SASHA, and SAPPHERE. *J Cardiovasc Magn Reson* 2014;**16**(Suppl. 1):O26.
- Bistoquet A, Oshinski J, Skrinjar O. Left ventricular deformation recovery from cine MRI using an incompressible model. *IEEE Trans Med Imaging* 2007;**26**:1136–53.

25. Bistoquet A, Oshinski J, Skrinjar O. Myocardial deformation recovery from cine MRI using a nearly incompressible biventricular model. *Med Image Anal* 2008;**12**: 69–85.
26. Mizuguchi Y, Oishi Y, Miyoshi H, Iuchi A, Nagase N, Oki T. Concentric left ventricular hypertrophy brings deterioration of systolic longitudinal, circumferential, and radial myocardial deformation in hypertensive patients with preserved left ventricular pump function. *J Cardiol* 2010;**55**:23–33.
27. Palmon LC, Reichel N, Yeon SB, Clark NR, Brownson D, Hoffman E et al. Intramural myocardial shortening in hypertensive left ventricular hypertrophy with normal pump function. *Circulation* 1994;**89**:122–31.
28. McLenachan JM, Dargie HJ. Ventricular arrhythmias in hypertensive left ventricular hypertrophy. Relationship to coronary artery disease, left ventricular dysfunction, and myocardial fibrosis. *Am J Hypertens* 1990;**3**:735–40.
29. MacIver DH, Adeniran I, Zhang H. Left ventricular ejection fraction is determined by both global myocardial strain and wall thickness. *J Clin Hypertens* 2015;**7**:113–8.
30. Treibel TA, Zemrak F, Sado DM, Banypersad SM, White SK, Maestrini V et al. Extracellular volume quantification in isolated hypertension—changes at the detectable limits? *J Cardiovasc Magn Reson* 2015;**17**:74.
31. Kuruville S, Janardhanan R, Antkowiak P, Keeley EC, Adenaw N, Brooks J et al. Increased extracellular volume and altered mechanics are associated with LVH in hypertensive heart disease, not hypertension alone. *JACC Cardiovasc Imaging* 2015;**8**:172–80.
32. Velagaleti RS, Gona P, Chuang ML, Salton CJ, Fox CS, Bleuse SJ et al. Relations of insulin resistance and glycemic abnormalities to cardiovascular magnetic resonance measures of cardiac structure and function: the Framingham Heart Study. *Circ Cardiovasc Imaging* 2010;**3**:257–63.

IMAGE FOCUS

doi:10.1093/ehjci/jew295

Online publish-ahead-of-print 24 December 2016

Evanescent atrial tumour after percutaneous coronary intervention

Ula Limon, Hilmi Kaplan, and Juan Luis Gutiérrez-Chico*

Department of Cardiology, Klinikum Frankfurt (Oder), Müllroser Chaussee 7, 15236 –Frankfurt (Oder), Müllroser Chaussee 7, 15236 – Frankfurt (Oder), Germany

* Corresponding author. Tel +49 (0) 3355 48 1454, +49 (0) 176 30585019, +34 615 319370. E-mail: juanluis.gutierrezchico@ictrea.es

A 75-year-old female patient consulted for shortness of breath over the last week. A rise in the serum levels of high-sensitivity TnT prompted a coronary angiography before a transthoracic echocardiogram (TTE) could be obtained. A severe stenosis in the proximal LCX underwent percutaneous coronary intervention (PCI).

The following day the patient kept on complaining about shortness of breath and a TTE unveiled a bulky tumour in the left atrium. The mass had heterogeneous echogenicity, oval shape, regular contour and a base of implantation on the lateral and inferior walls of the atrium, as depicted in transoesophageal echocardiogram (A, B; Supplementary data online, Videos 1–4) and multi-slice computed tomography (C). Intraatrial masses of similar characteristics have been reported as hematomas complicating PCI of chronic total occlusions or different ablation procedures. A careful review of the PCI, unravelled that the operator chose a core-to-tip hydrophilic-coated wire (PILOT 50, Abbott Vascular, Santa Clara, CA) and placed it in an atrial branch of the LCX (D, asterisk; Supplementary data online, Video 5). Inappropriate manipulation led to inadvertent progression of the wire deep into the atrial branch over the intervention (Supplementary data online, Video 6). The final angiographic recording showed clear contrast staining in the atrial wall (D, arrows; Supplementary data online, Video 7), thus strongly suggesting the diagnosis of iatrogenic haematoma. The tumour was regressive in serial imaging controls and it completely vanished 2 months after the initial diagnosis (A–C, FU subpanels; Supplementary data online, Videos 8–10).

This case underscores the importance of an appropriate material selection and a refined interventional technique to avoid potentially life-threatening complications.

Supplementary data are available at *European Heart Journal—Cardiovascular Imaging* online.

